ANGULAR DISTRIBUTIONS OF $\bar{p}p \to \pi^o\pi^o$ AND $\bar{p}p \to \pi^o\eta^o$ AT 1.752 GeV/c*

C. DeMarzo, L. Guerriero, F. Posa, E. Vaccari, F. Waldner
Bari University, Bari Italy+.

R.E. Lanou (Jr.), J.T. Massimo, R.K. Thornton
Brown University, Providence, R.I. 02912, U.S.A.++.

D.S. Barton, B.A. Nelson, M. Marx, D.C. Peaslee°, L. Rosenson
Massachusetts Institute of Technology and Laboratory for Nuclear Science
Cambridge, Mass. 02139, U.S.A.++.

(Presented by L. Rosenson)

We present here preliminary results of an optical spark chamber experiment to measure gamma ray final states of proton-antiproton annihilations. Angular distributions are given for $\bar{p}p \to \pi^o\pi^o$ and $\bar{p}p \to \pi^o\eta^o$ at 1.752 GeV/c incident momentum.

The experiment was performed in a partially separated antiproton beam at the brookhaven National Laboratory AGS. The beam included two 15 foot D.C. separators and a 12 element tagging hodoscope at the momentum focus, giving us a momentum resolution capability of 0.4%. After separation the beam contained equal numbers of $\bar{p}$ and π^-. Using a 16 meter flight path we were able to achieve better than a 10^{-3} rejection rate of pions. The beam was then incident on a 10 cm liquid hydrogen target which was surrounded by a two layer scintillation counter hodoscope covering the entire solid angle. The first layer vetoed all events with charged secondaries. Between the layers was one radiation length of lead in order to convert gamma rays. The second layer consisted of 17 counters designed to be sensitive to two body correlations. A good trigger was required to have a count in two counters - one forward, one backward, and on the same azimuth (Fig. 1). This strongly biased our trigger against the neutral baryonic reactions like $\bar{n}n$ and $\bar{n}n\pi^o$, and towards two body states like $\pi^o\pi^o$ and $\pi^o\eta^o$. For example, the $\bar{n}n$ triggering efficiency was $\simeq 10^{-3}$ while that for $\pi^o\pi^o$ was $\simeq 0.4$. If an event satisfied the logic we then fired the spark chambers.

---

* Part of this work has been carried out at the Brookhaven National Laboratory, Uption, N.Y. 11973, U.S.A.

+ Work supported by the USA-Italy Scientific Cooperation Program and the Istituto Nazionale di Fisica Nucleare.

++ Work supported by the U.S. Atomic Energy Commission under Contracts No. AT(11-1)-3130TB and AT(11-1)-3069.

o Permanent address: Australian National University, Canberra, Australia.

The six spark chambers covered the entire solid angle and presented a minimum of eight radiation lengths in 80 gaps for converting and detecting the gamma ray showers (Fig. 2).

In the course of the experiment we took approximately 750,000 pictures at 20 equally spaced energies between 1.1 and 2.0 GeV/c with tagging to invariant mass bins of $\approx$ 2.5 MeV.

It is a kinematical property of massive particles decaying into gamma ray pairs that the distribution of the opening angle, Θ, between the gammas is characterized by a sharp minimum angle with most of the events piling up near this minimum[1]. This minimum is a function only of the velocity, β, of the decaying particle, which in the center of mass of a two body event is unique. We have $\cos\frac{\Theta_{min}}{2} = \beta$. At 1.752 GeV/c, Θ_{min} for π^o from $\bar{p}p \to \pi^o\pi^o$ is 13o; for $\bar{p}p \to \pi^o\eta^o$, Θ_{min} is 13.8^o for the π^o and 52.2^o for η^o.

Because of the efficiency of our system for detecting gamma rays, more than 95% of $\pi^o\pi^o$ and $\pi^o\eta^o$ events in which the π^o and η^o decay via two gamma are detected as either four gamma or three gamma events. Figs. 3 and 4 show all pairs of center of mass opening angles for all three or four gamma events. Prominent in both are the π^o peaks. To find the two body events we display on a scatter plot the smallest opening angle for each event versus the remaining opening angle (Fig. 5). The accumulation at the minimum opening angle for both pairs at the π^o angle is apparent. There is also a clear accumulation at the π^o angle.

We have one more kinematic variable in a two body process, namely the angle between directions of the decaying particles. In the center of mass these directions should have a relative angle of 180^o. Using the bisector of the pairs as an approximation and making a cut at 15^o on the angle between one bisector and the reflection of the other, one sees a dramatic enhancement of signal to noise (Fig. 6). In practice one can do better by treating the sample as though they were all $\pi^o\pi^o$ or $\pi^o\eta^o$ events. Under these hypotheses one can calculate for each pair of gammas from an assumed π^o or η^o the two possible directions for the π^o or η^o. there are two possible solutions, symmetrically disposed on either side of the bisector, since we do not distinguish which gamma has the higher energy. For each event we select the two directions which are closest to 180^o apart. In Fig. 7 we show the reflected relative angle distribution for pairs passing cuts on the opening angle (smaller $\Theta < 21^o$, larger $\Theta < 30^o$). Also shown is the relative angle distribution for three gamma events, which we determine between the solution of the pair (with $\Theta < 30^o$) closest to 18^o to the odd gamma. For the three gamma events we display the smallest opening angle versus the relative angle to show the accumulation at the $\pi^o\pi^o$ region (Fig. 8).

There is some contamination of background in both of these samples, which arise from systems of higher multiplicity, e.g., three π^o or four π^o, and which are not detected in their entirety in the equipment. To estimate this background we generate events by eliminating short gammas from observed events having five or more gammas. These are most probably the gammas that would be lost due to detection inefficiencies and would give rise to lower multiplicity events. Treating those events that become four gammas under this operation as a background sample we normalize to the region outside the $\pi^o\pi^o$ and $\pi^o\eta^o$ regions on the scatter plot of the data events and perform a subtraction. For the three gamma events we use the opening angle versus the relative angle scatter plot to ascertain the background.

For the three gamma $\pi^o\pi^o$ events there is an additional background from the $\pi^o\eta^o$ events where one of the η^o gammas is missed. In fact ≃ one half of the number that appear in the $\pi^o\eta^o$ region would fall into $\pi^o\pi^o$ region. This is calculated using a Monte Carlo program. The final raw angular distributions for $\pi^o\pi^o$ and $\pi^o\eta^o$ events passing the cuts are shown in Figs. 9, 10 and 11. We use as an estimate of the polar angle for each event the direction obtained by appropriately averaging the two space vectors representing the $\pi^o\pi^o$ or $\pi^o\eta^o$ for each event.

In order to correct these distributions for triggering biases and efficiency, geometric detection inefficiencies and experimental resolution, we use a Monte Carlo simulation program. To check the results of this program we have used several calibrations. First, we are able to predict correctly the number of gamma rays converting in our lead scintillator hodoscope, for a given number of gamma rays incident upon the detector, by determining the number of gammas as a function of distance into the chamber and extrapolating back to the beginning to find the excess over an exponential rise. Second, we can predict the number of counters fired and compare with the data, since this is encoded on each picture. Third, we are able to predict the number of events which are visible as four gamma or three gamma events as a function only of an effective low energy cut-off on visible gammas in the chambers, which we can adjust to fit the data. Fourth, the Monte Carlo events spread with the experimental measurement errors agrees with the data in opening angle distribution, relative angle distribution, etc. (see Fig. 7).

To reconstruct angular distributions from the raw data we need to generate with the Monte Carlo a matrix which gives the probability for detecting an event in dx' at $x' = \cos\Theta'$ if it actually occurred in dx at $x = \cos\Theta$. To do this we define a density $M(x,x')$ [5] such that the observed distribution $n'(x')$ can be gotten from the true parent distribution $n(x)$. The results of these fits are given in Fig. 12 for the $\pi^o\pi^o$. It is encouraging that the fitted distributions and the normalization come out so similar to each other in the three gamma and four gamma cases, especially since the raw samples are so dissimilar (Figs. 9, 10). In Fig. 13 we show the results of the fit to the $\pi^o\eta^o$ sample. Because of the symmetries of the two processes the differential cross section of both $\bar{p}p \to \pi^o\pi^o$ and $\bar{p}p \to \pi^o\eta^o$ are restricted to even Legendre polynomial expansions. We fit for successively increasing values of L_{max} and stopped adding terms when the probability for the fit reached reasonable values and stabilized. In Fig. 14 we show the situation for the $\pi^o\pi^o$ case. We accepted $L_{max} = 8$ and rejected $L_{max} = 10$ because the a_{10} that was required was consistent with 0.

The integrated cross section for $\bar{p}p \to \pi^o\pi^o$ at 1.752 GeV/c is 12.85 ± 1.2 μb, where the error is statistical. There is an additional overall uncertainty in the normalization, which we estimate at this time to be ≃ 10%.

In Table 1 we list the properly normalized coefficients a_ℓ in the expansion

$$\frac{d\sigma}{d\Omega} = \sum_{\ell=0}^{L_{max}} a_\ell P_\ell(x)$$

Also listed are the coefficients in a similar expansion for the process $\bar{p}p \rightarrow \pi^+\pi^-$ from the data of Eisenhandler et al. [(2)]. We have averaged the fits of these authors to their data at 1.70 and 1.80 GeV/c to compare with our data at 1.752 GeV/c.

If we represent the two π annihilation process by two I spin amplitudes, M_0 and M_1,

then $$M_{+-} = M_0 + M_1$$

and $$M_{00} = M_0$$

then $$\frac{d\sigma_{+-}}{d\Omega} = |M_0|^2 + |M_1|^2 + 2\text{Re}M_0M_1^*$$

$$\frac{d\sigma_{00}}{d\Omega} = |M_0|^2$$

Initial spin state indices and averages have been suppressed in the above. Since the dipion state must be symmetric, including the I spin variable, the amplitudes M_1 and M_0 must be composed of odd and even spherical harmonics respectively. This implies that $|M_1|^2$ and $|M_0|^2$ have purely even expansions in Legendre polynomials and only the interference term gives rise to the odd terms in the expansion of the cross section.

Since the $\pi^0\pi^0$ measurement determines $|M_0|^2$ separately, we can subtract it from the $\pi^+\pi^-$ expansion and the remaining odd and even terms are separately $|M_1|^2$ and $2\text{Re}M_0M_1^*$. This separation is shown in the last two columns of Table 2 and the separate angular functions are displayed in Fig. 15.

The most outstanding feature of the Legendre polynomial fits to the $\pi^0\pi^0$ data is the large a_8 coefficient. The other coefficients, aside from a_0, which basically determines the total cross section for the reaction, are all small. Due to the fact that the two pi annihilation takes place from the triplet $\bar{p}p$ states only, the general form of the amplitude contains only incoherent sums of spherical harmonics with $m = 0$ and ± 1[(3)]. This fact, coupled to the obviously related observation that the differential cross section has a very strong dip-peak structure with almost hard zeros tempts one to try to interpret the data in terms of the simplest amplitude possible.

The results of an incomplete search for various combinations of functions which could fit the data are given in Table 2. In fact we found that we had very little freedom to chose various combinations of functions and we reproduce our best almost unique solutions. The following comments are in order: $|M_0|^2$ is quite adequately describable as $|aY_2^0 + bY_4^0|^2$ with a and b very close to 180^0 out of phase. It will be interesting to see whether this analysis holds up at neighboring energies and whether either a or b varies rapidly with energy as would happen if there were an I = 0, J = 2 or 4 resonance in this region. We note in passing that the energy of this experiment is close to the center of the broad maximum in the $\bar{p}p$ and $\bar{p}n$ total cross sections(4) that has been suggested to be due to both an I = 0 and I = 1 resonance in this energy region. The momentum bite covered by this experiment was ≃ 85 MeV/c and each event was tagged to ± 3.5 MeV/c incident momentum. We searched for possible variation in the angular distribution across this region (≃ 30 MeV in mass) and within the limited statistics available we see no strong variation in the angular distribution. (See Fig. 16). In this connection, the reaction $\bar{p}p \rightarrow \pi^0\eta^0$ is pure $I^G = 1^-$ and seems to have a very different angular momentum composition than the I = 1 part of $\bar{p}p \rightarrow \pi^+\pi^-$ (which is $I^G = 1^+$). (See Figs. 13 and 15).

The $|M_1|^2$ angular distributions turned out to yield somewhat less satisfactory solutions after a similar search. While we get very good reproductions of the angular distributions with the parameters indicated in Table 1, the coefficients are not consistent with those that would arise from a proper amplitude squared. There is considerable sensitivity to the relative normalization of the two experimental input samples, particularly with regard to the magnitude of the coefficients of the $Y_3^1 Y_5^1$ and $Y_5^1 Y_1^1$ terms.

In conclusion, the first angular distributions we have obtained in these neutral two body processes show great promise for aiding in the understanding of the rich structure in the $\bar{p}p$ annihilations. Over the next year we will have substantially more data and will attempt a more thorough analysis.

We gratefully acknowledge the expert technical assistance of Mr. T. Lyons and his group at Brookhaven and Mr. A. Distante and his group at Bari and the excellent work of our various scanning staffs. We wish to thank Messrs. W. Aitkenhead, J. Butler and S. Redner for their assistance during the construction, running and preliminary data analysis.

REFERENCES

1) B. Rossi, High Energy Particles (Prentice Hall, Inc., Englewood Cliffs, New jersey, 1962), p. 198.

2) E. Eisenhandler et al., Phys. Lett. B47, 531 (1973), and A. Astbury, private communication.

3) H. Nicholson et al., Phys. Rev. D7, 2585 (for a general expression for $d\sigma/d\Omega$ for 2 π annihilation). (1973).

4) R.J. Abrams et al., Phys. Rev. D1, 1917 (1970).

5) F. Bulos et al., Phys. Rev. 187, 1827 (1969).

TABLE 1

Legendre coefficient expansions for $\pi^o\pi^o$ and $\pi^-\pi^+$ with isotopic spin decompositions

$$M^{+-} = M^o + M^1$$

$$M^{oo} = M^o$$

$$M^o(\Theta) = M^o(\pi-\Theta) \qquad M^1(\Theta) = -M^1(\pi-\Theta)$$

$$\frac{d\sigma}{d\Omega}^{+-}(\Theta) = |M^o|^2 + |M^1|^2 + 2\,\mathrm{Re}\,M^o M^{1*}$$

$$= \sum_{\ell\,\mathrm{even}} a_\ell^o P_\ell + \sum_{\ell\,\mathrm{even}} a_\ell^1 P_\ell + \sum_{\ell\,\mathrm{odd}} a_\ell^{o1} P_\ell$$

$$\frac{d\sigma}{d\Omega}^{oo}(\Theta) = |M^o|^2 = \sum_{\ell\,\mathrm{even}} a_\ell^o P_\ell$$

$$\frac{d\sigma}{d\Omega}^{+-} - \frac{d\sigma}{d\Omega}^{oo} = |M^1|^2 + 2\,\mathrm{Re}\,M^o M^{1*}$$

$$\sum_{\ell\,\mathrm{even}} a_\ell^1 P_\ell + \sum_{\ell\,\mathrm{odd}} a_\ell^{o1} P_\ell$$

$$\sigma_{I=1}^{tot} = \int_{4\pi} \left(\frac{d\sigma}{d\Omega}^{+-} - \frac{d\sigma}{d\Omega}^{oo}\right) d\Omega = \sigma^{+-} - 2\sigma^{oo}$$

$$\sigma_{I=0}^{tot} = 3\sigma^{oo}$$

1.75 BeV/c Legendre Coefficients

ℓ	a_ℓ^o	$a_\ell^o + a_\ell^1 + a_\ell^{o1}$	a_ℓ^{o1}	a_ℓ^{o1} μb/sr
0	2.05 ± .19	7.85 ± .17	5.8 ± .23	
1		.67 ± .34		.67 ± .34
2	-.15 ± .43	-.13 ± .44	.2 ± .55	
3		2.03 ± .52		2.03 ± .52
4	.78 ± .65	0.1 ± .66	-.68 ± .83	
5		5.90 ± .65		5.90 ± .65
6	-1.46 ± .73	5.57 ± .69	7.03 ± .89	
7		-.32 ± .73		-.32 ± .73
8	4.32 ± .89	12.8 ± .8	8.48 ± 1.06	
9		.44 ± .8		.44 ± .8
10		-2.46 ± .92	-2.46 ± .92	

Amplitude decomposition of isotopic spin angular distributions

Amplitude Analysis
(in μb/sr)

$$|M_o|^2 = (39.3\pm6)|Y_{40}|^2 - (59.6\pm7.7)|Y_{40}Y_{20}| + (18.3\pm7)|Y_{20}|^2$$

Prob(X^2) ≃ 65%

$$|M_1|^2 = (22.17\pm8)|Y_{51}|^2 + (64.3\pm8.9)|Y_{31}|^2 + (80.3\pm7.9)|Y_{30}|^2 - (130.6\pm10.7)|Y_{51}Y_{31}| + (117.4\pm28.7)|Y_{51}Y_{11}|$$

Prob(X^2) ≃ 35%

$$2\mathrm{Re}|M_1M_o^*| = (53.9\pm16)|Y_{40}Y_{10}| - (38.7\pm12)|Y_{20}Y_{10}| + (31.0\pm7.5)|Y_{20}Y_{30}| - (3.3\pm7.5)|Y_{40}Y_{30}|$$

Prob(X^2) ≃ 75%

FIGURE CAPTIONS

1) Arrangement of trigger counters and logic table.

2) Spark chamber system.

3) Opening angle distribution - four gamma events, 6 per event.

4) Opening angle distribution - three gamma events, 3 per event.

5) Scatter plot of smallest opening angle versus remaining opening angle, four gamma events.

6) Same as Fig. 5 with bisector-bisector angle greater than 165^o.

7) Relative angle distribution for three and four gamma events after π^o opening angle cuts.

8) Smallest opening angle versus relative angle, three gamma events.

9) Raw angular distribution $\pi^o\pi^o$ four gamma events.

10) Raw angular distribution $\pi^o\pi^o$ three gamma events.

11) Raw angular distribution $\pi^o\eta^o$.

12) Fitted angular distribution $\pi^o\pi^o$, showing fits to three gamma, four gamma and combined samples.

13) Fitted angular distribution $\pi^o\eta^o$.

14) χ^2 versus number of coefficients for $\pi^o\pi^o$.

15) Isospin angular distributions.

16) $\pi^o\pi^o$ angular distribution across momentum byte by hodoscope

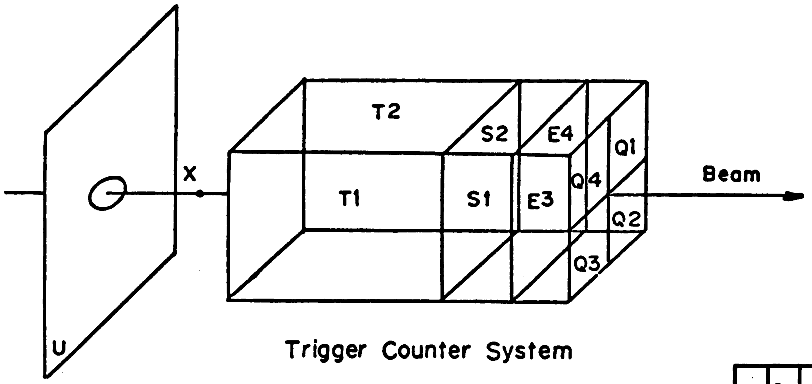

Trigger Counter System

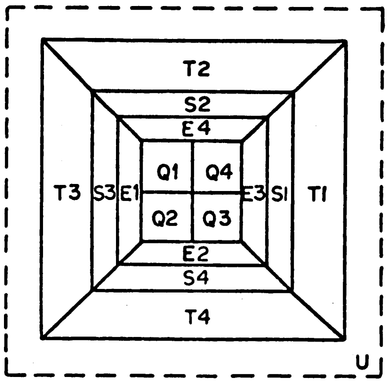

View looking downstream from X

	S1 T1	S2 T2	S3 T3	S4 T4	S1	S2	Q	E
Q1	X			X				
Q2	X	X						
Q3		X	X					
Q4			X	X				
E1	X							
E2		X						
E3			X					
E4				X				
S3					X			
S4						X		
U							X	X

logic pair

Trigger Counters

Fig. 1

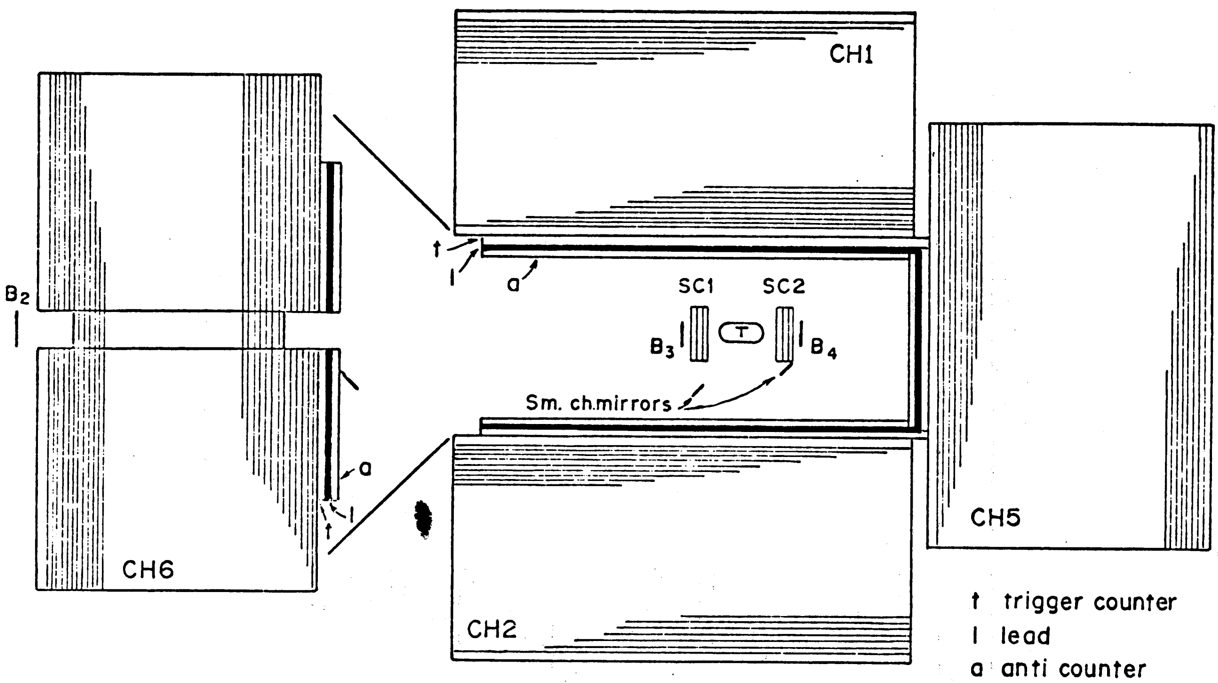

Fig. 2

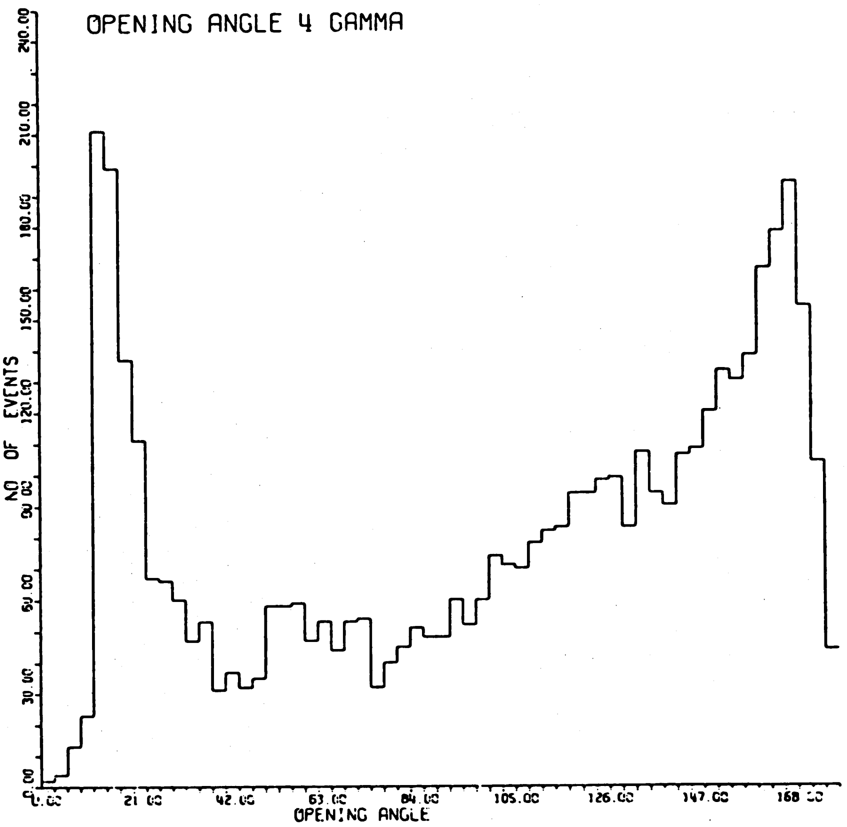
OPENING ANGLE 4 GAMMA
NO OF EVENTS
OPENING ANGLE
21.00
42.00
63.00
84.00
105.00
126.00
147.00
168.00
30.00
60.00
90.00
120.00
150.00
180.00
210.00
240.00

Fig. 3

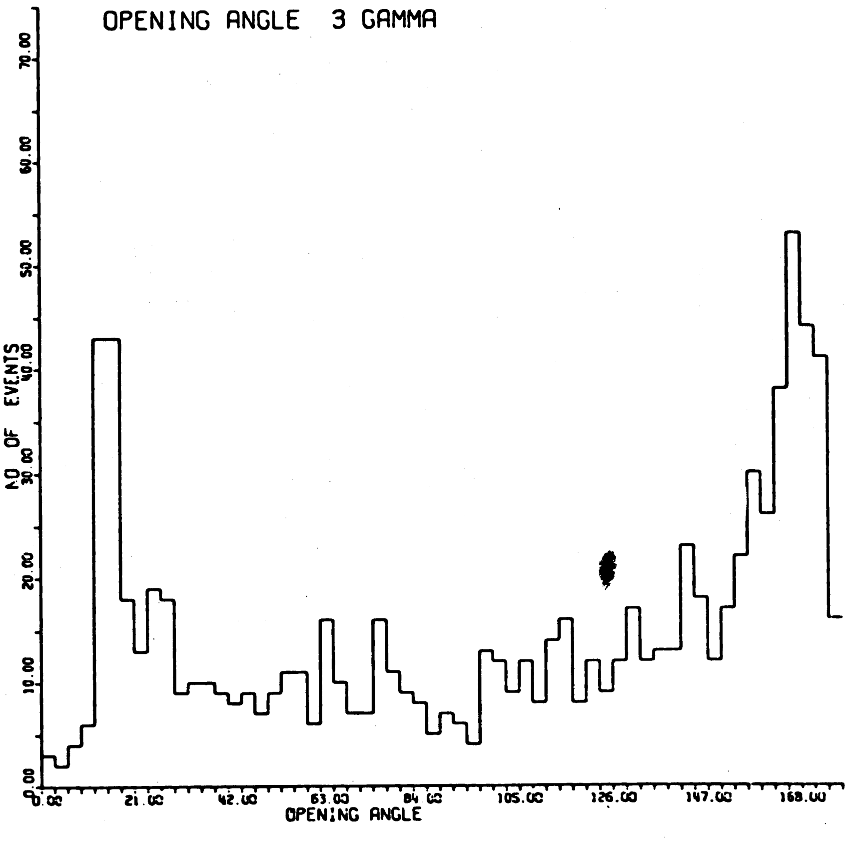
OPENING ANGLE 3 GAMMA
NO OF EVENTS
OPENING ANGLE
0.00
21.00
42.00
63.00
84.00
105.00
126.00
147.00
168.00
10.00
20.00
30.00
40.00
50.00
60.00
70.00

Fig. 4

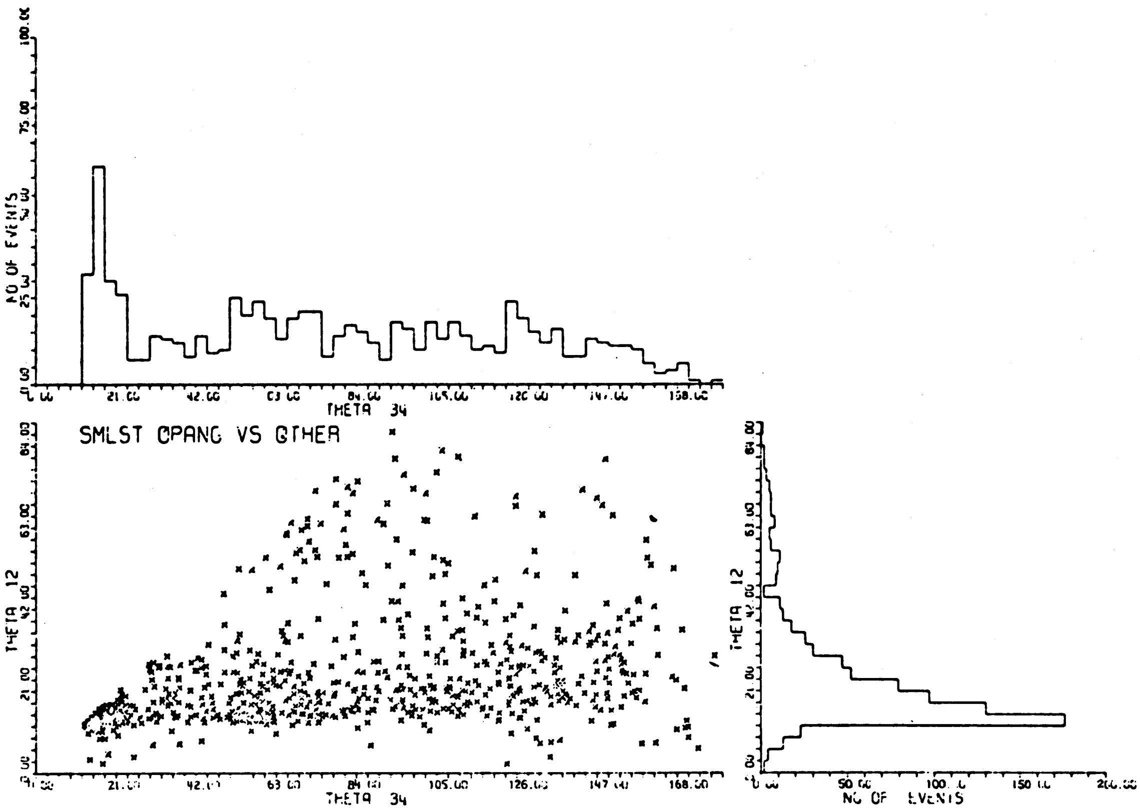
NO OF EVENTS
THETA 34
SMLST OPANG VS OTHER
THETA 12
NO OF EVENTS

Fig. 5

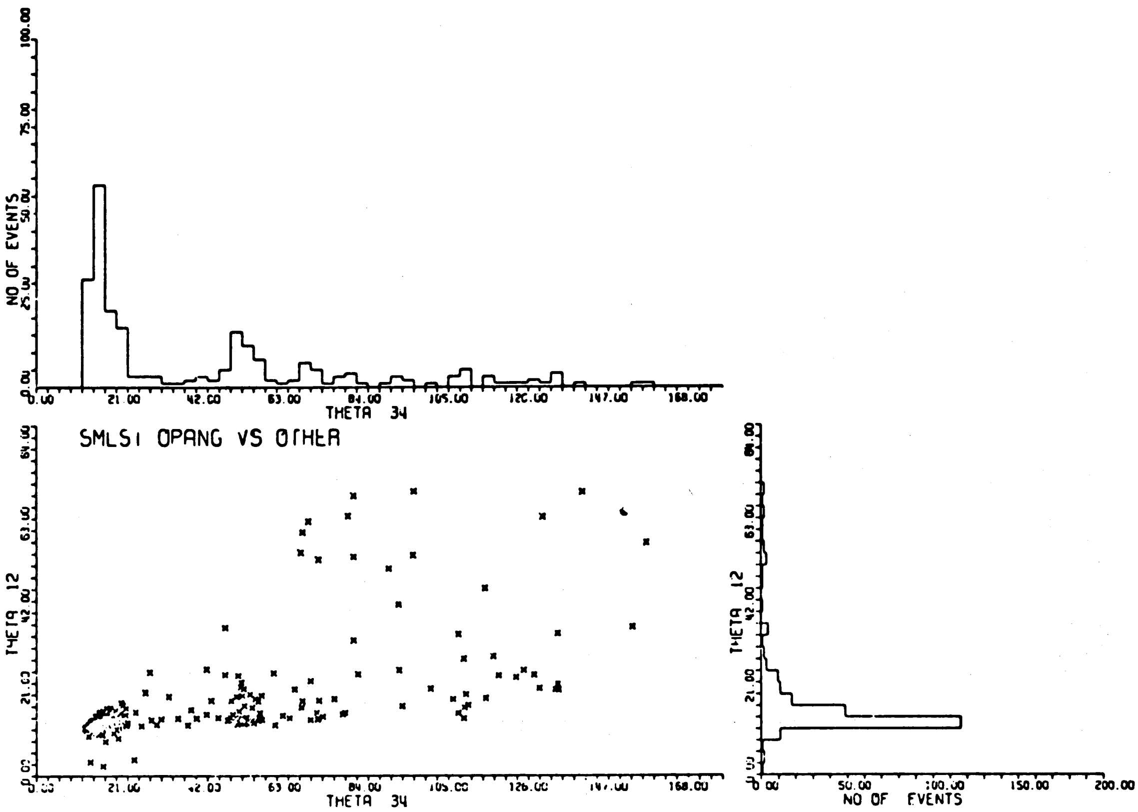
NO OF EVENTS
THETA 34
SMLST OPANG VS OTHER
THETA 12
NO OF EVENTS

Fig. 6

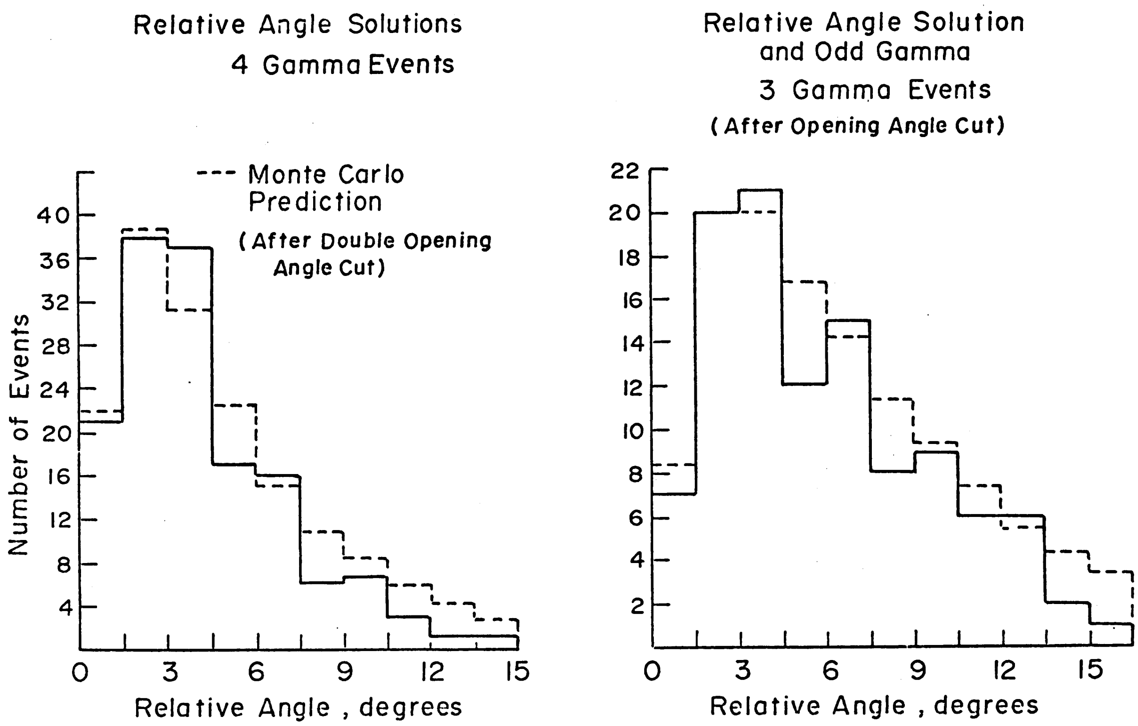
Relative Angle Solutions
4 Gamma Events
--- Monte Carlo Prediction
(After Double Opening Angle Cut)
Number of Events
40
36
32
28
24
20
16
12
8
4
0
3
6
9
12
15
Relative Angle , degrees
Relative Angle Solution and Odd Gamma
3 Gamma Events
(After Opening Angle Cut)
22
20
18
16
14
12
10
8
6
4
2
0
3
6
9
12
15
Relative Angle , degrees

Fig. 7

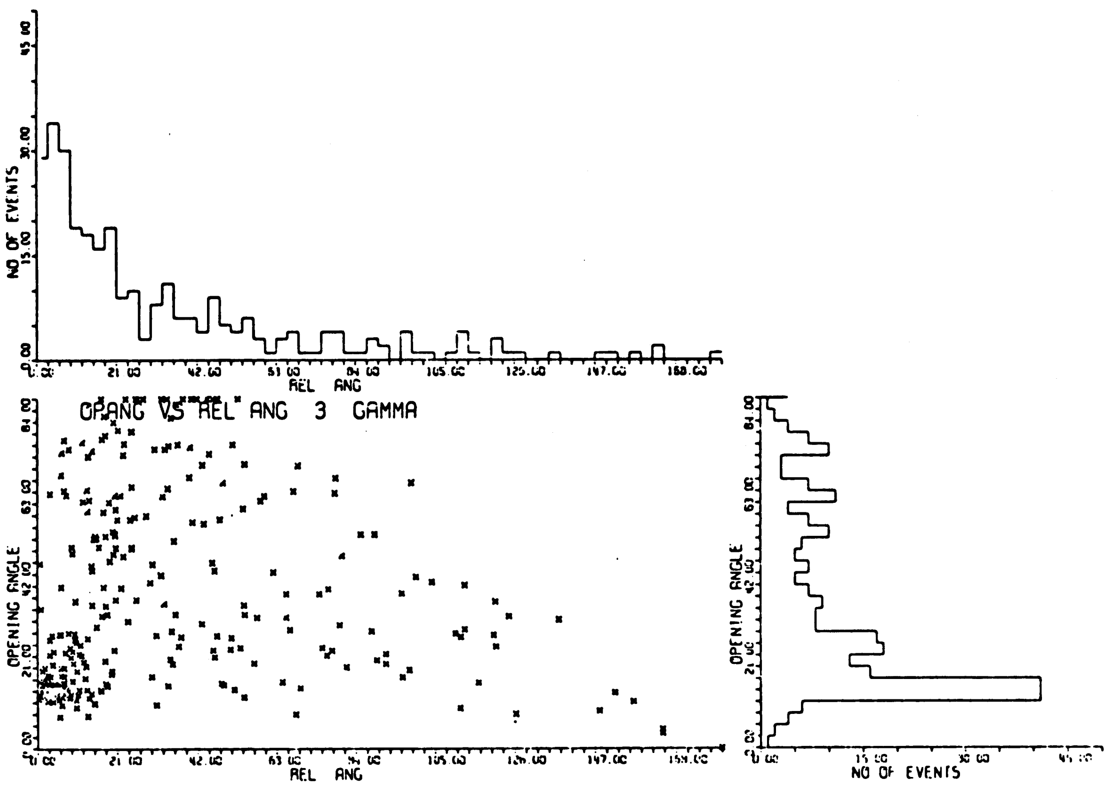
NO OF EVENTS
REL ANG
OPANG VS REL ANG 3 GAMMA
OPENING ANGLE
REL ANG
OPENING ANGLE
NO OF EVENTS

Fig. 8

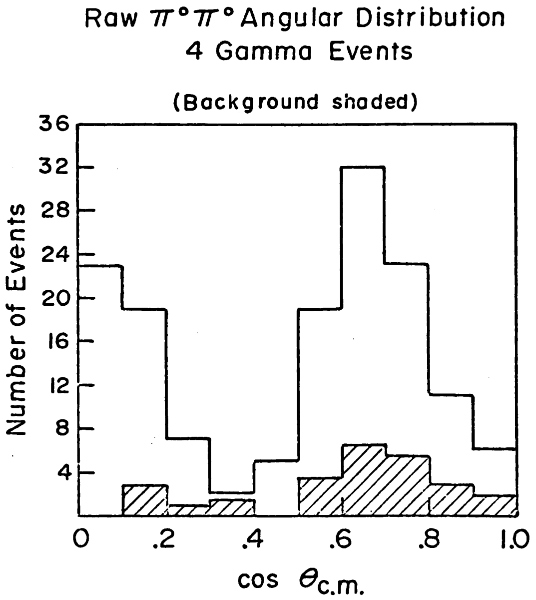

Fig. 9

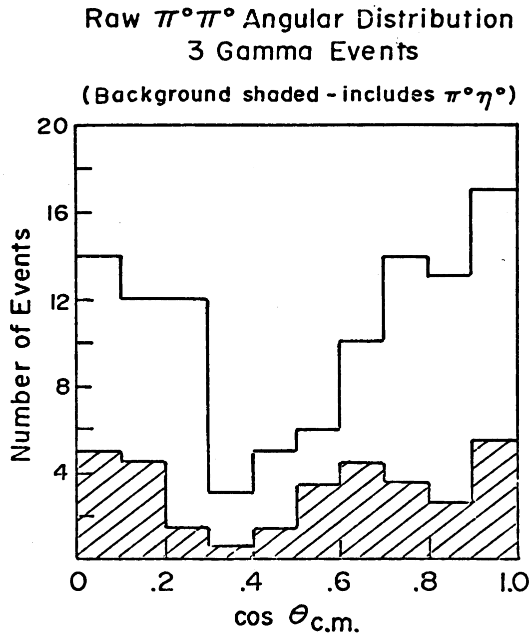

Fig. 10

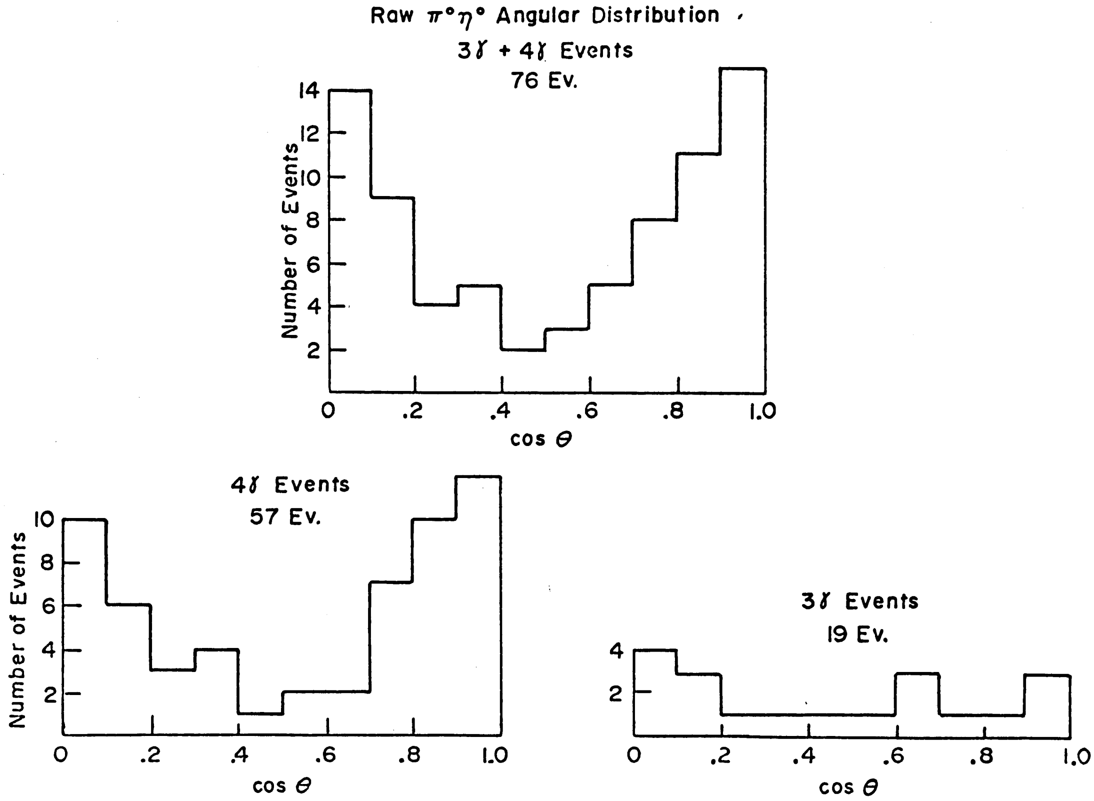

Fig. 11

$\pi^\circ\pi^\circ$ Fitted Parent Distributions
(Histogram shows $3\gamma + 4\gamma$ raw data)

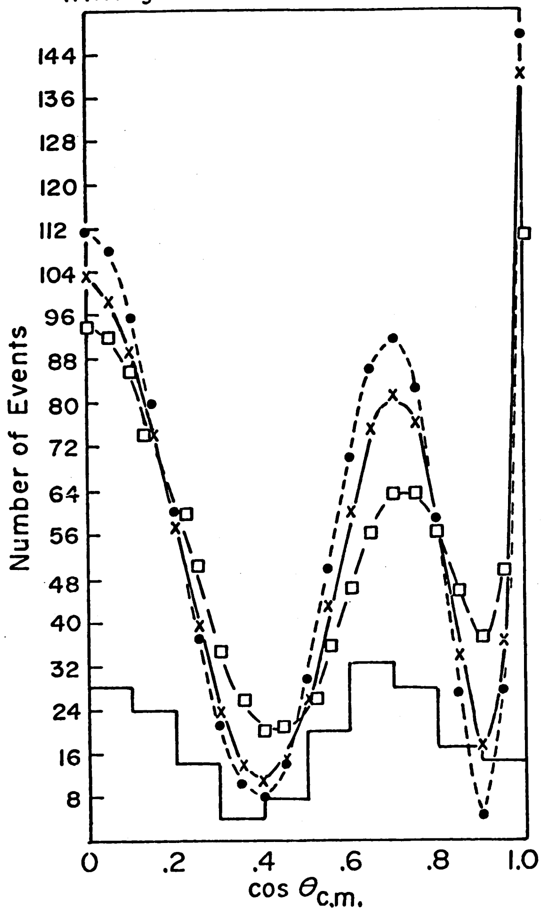

x $3\gamma + 4\gamma$ Parents $C_o = 520.6 \pm 37.9$ Prob $(\chi^2) = .55$
• 4γ Parents $C_o = 540.6 \pm 49.8$ Prob $(\chi^2) = .50$
□ 3γ Parents $C_o = 519.6 \pm 60.0$ Prob $(\chi^2) = .50$

Fig. 12

$\pi^\circ\eta^\circ$ Folded Angular Distribution
1.752 GeV/c

$$\frac{d\sigma}{d\Omega} = (2.25 \pm .26)\,P_0 + (1.16 \pm .66)\,P_2 + (3.1 \pm .85)\,P_4\ \mu b/sr$$
Prob $(\chi^2) = 20\%$

$\sigma_{\pi\eta} = 28.3 \pm 3.2\ \mu b = 4\pi a_0$
(includes~10% background)

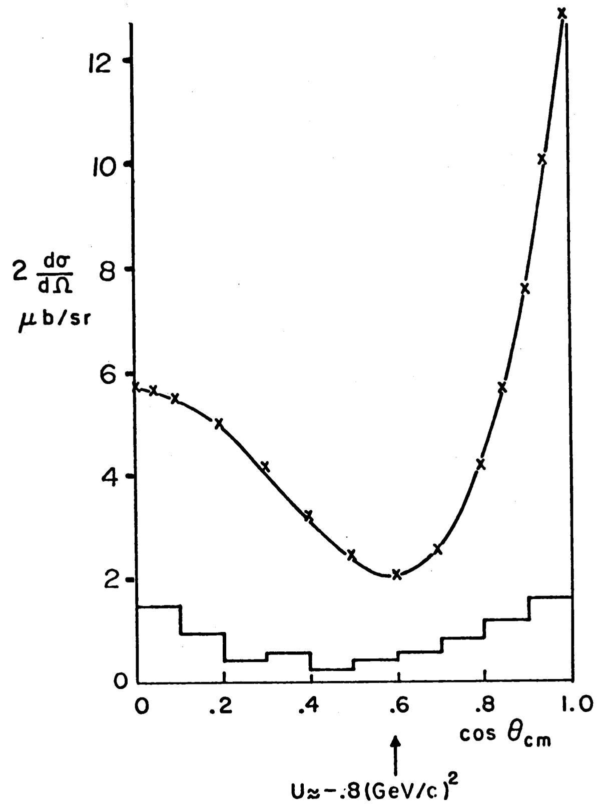

Fig. 13

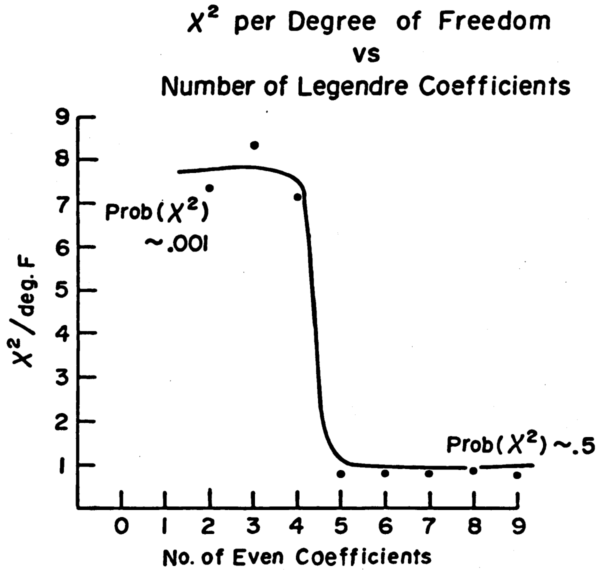
χ^2 per Degree of Freedom
vs
Number of Legendre Coefficients
χ^2/deg. F
Prob(χ^2) ~.001
Prob(χ^2) ~.5
0 1 2 3 4 5 6 7 8 9
No. of Even Coefficients

Fig. 14

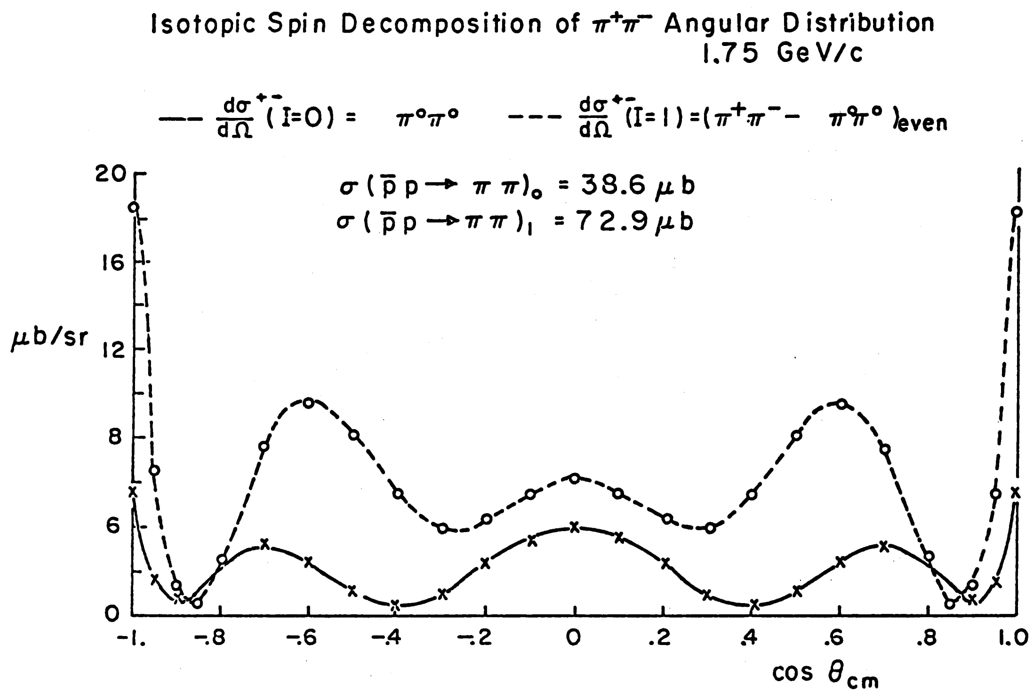
Isotopic Spin Decomposition of $\pi^+\pi^-$ Angular Distribution
1.75 GeV/c
$\frac{d\sigma^{+-}}{d\Omega}(I=0) = \pi^0\pi^0$
$\frac{d\sigma^{+-}}{d\Omega}(I=1) = (\pi^+\pi^- - \pi^0\pi^0)_{even}$
$\sigma(\bar{p}p \rightarrow \pi\pi)_0 = 38.6\ \mu b$
$\sigma(\bar{p}p \rightarrow \pi\pi)_1 = 72.9\ \mu b$
μb/sr
$\cos\theta_{cm}$

Fig. 15

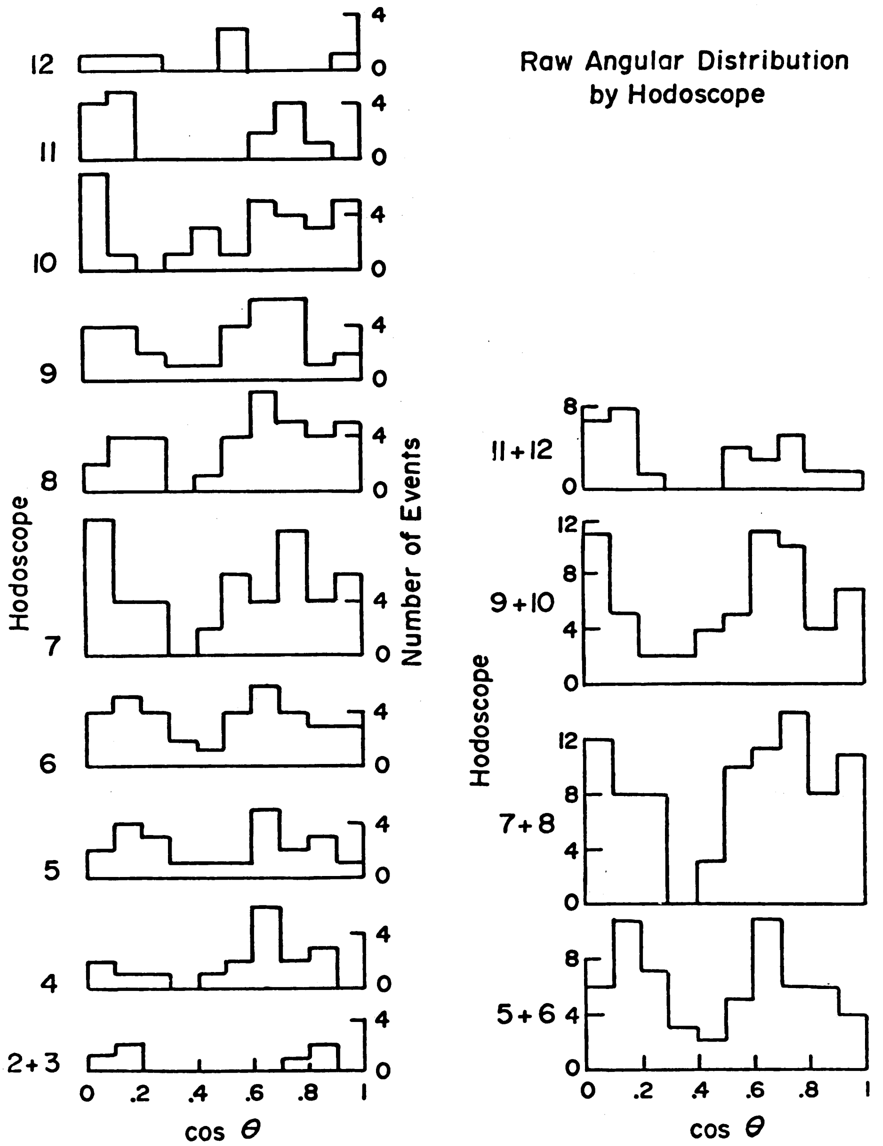
Raw Angular Distribution
by Hodoscope
Hodoscope
Number of Events
12
11
10
9
8
7
6
5
4
2+3
11+12
9+10
7+8
5+6
0
4
8
12
0
.2
.4
.6
.8
1
cos θ

Fig. 16

D I S C U S S I O N

- *Lillestøl:*

  Can you always pick the γ-pair with the smallest opening angle?

- *Rosenson:*

  No, not always. There are sometimes troubles with bremsstrahlung and so on.

- *Lillestøl:*

  Do you lose many events by picking the wrong combination?

- *Rosenson:*

  No, only a few per cent.